The controllable synthesis of nanoporous $SrTiO_3$ by an ultrasound irradiation approach

2011 Smart Mater. Struct. 20 065002

(http://iopscience.iop.org/0964-1726/20/6/065002)

IOP PUBLISHING SMART MATERIALS AND STRUCTURES
Smart Mater. Struct. **20** (2011) 065002 (5pp) doi:10.1088/0964-1726/20/6/065002

The controllable synthesis of nanoporous $SrTiO_3$ by an ultrasound irradiation approach

Wanquan Jiang[1,4], **Wei Zhu**[1], **Chuanxia Jiang**[1], **Xueping Zhang**[1], **Shouhu Xuan**[2], **Xinglong Gong**[2,4] and **Zhong Zhang**[3]

[1] Department of Chemistry, University of Science and Technology of China (USTC), Hefei 230026, People's Republic of China
[2] CAS Key Laboratory of Mechanical Behavior and Design of Materials, Department of Modern Mechanics, USTC, Hefei 230027, People's Republic of China
[3] National Center for Nanoscience and Technology, Beijing 100080, People's Republic of China

E-mail: jiangwq@ustc.edu.cn and gongxl@ustc.edu.cn

Received 25 December 2010, in final form 8 April 2011
Published 3 May 2011
Online at stacks.iop.org/SMS/20/065002

Abstract
In this paper, nanoporous strontium titanate ($SrTiO_3$) with controllable morphologies was prepared by a simple and rapid ultrasound irradiation method. $SrTiO_3$ particles were synthesized by the hydrolysis of strontium alkoxide in an alcohol/water solution and the morphology was controlled by adjusting the reaction pH value. A possible formation mechanism for the nanoporous $SrTiO_3$ is proposed and the relevant influence of parameters is discussed. The chemical composition, porosity, microstructure and surface morphology of products were characterized by x-ray diffraction (XRD), the nitrogen adsorption–desorption method, scanning electron microscopy (SEM) and transmission electron microscopy (TEM). Nanoporous $SrTiO_3$ can be used as the precursor for an electrorheological fluid and experimental results indicated that the as-prepared $SrTiO_3$ electrorheological fluid (ERF) exhibited high shear stress and showed shear thinning behavior.

1. Introduction

Strontium titanate ($SrTiO_3$), with its excellent dielectric, ferroelectric and photoelectric properties, has been extensively documented as a material for oxygen gas sensors, photocatalysis and photoelectrodes [1–5]. Over the past few decades, much research about the synthesis of $SrTiO_3$ nanocrystals with different nanostructures, such as spheres, nanotubes, nanorods and nanowires [6–9], has been reported. Among various reported nanomaterials, porous materials exhibit important characteristics, such as a large surface area and a nanosize porous structure [10]. These characteristics make them widely used in photoelectronics, catalytic reactions, semiconductors and so on [11, 12]. Therefore, studies on the controllable synthesis of nanoporous $SrTiO_3$ are of great interest and are actively being pursued.

Up to now, many methods have been developed for the preparation of mesoporous and nanoporous $SrTiO_3$. Recently, Wang *et al* developed a general hydrothermal method to synthesize porous crystalline TiO_2, $SrTiO_3$ and $BaTiO_3$ spheres [13]. In their method, amorphous TiO_2 particles and strontium (barium) hydroxide hydrates were used as the raw materials and this reaction was conducted in a Teflon-lined stainless steel autoclave at a high temperature. The combustion synthesis method was also applied to the preparation of $SrTiO_3$ [14, 15]. Due to their wide applications, it is necessary and important to develop a simple approach to synthesize $SrTiO_3$ materials with a nanoporous nature.

The ultrasound irradiation method has proved to be a useful technique in the synthesis of materials with unusual and tailored properties [16, 17]. The chemical effects of ultrasound arise from acoustic cavitations, that is the formation, growth and implosive collapse of bubbles in the liquid. During cavitation, bubble collapse provides localized hot-spots with

---

[4] Authors to whom any correspondence should be addressed.

transient temperatures of 5000–25 000 K, pressures of about 1800 atm, and heating and cooling rates in excess of 1010 K s^{-1} [18]. The extreme conditions attained during bubble collapse have been exploited for the synthesis of various composites and its applications have been successfully demonstrated in nanoparticle preparation [19–21]. Through the ultrasound irradiation approach, amorphous iron powder of highly catalytic activity was prepared by Suslick [19]. It can catalyze the Fischer–Tropsch hydrogenation of carbon monoxide and the hydrogenolysis and dehydrogenation of saturated hydrocarbons. Hydrated amorphous $FePO_4$, which exhibited high discharge capacities, was also synthesized by a sonochemical reaction method [22]. However, reports on the synthesis of $SrTiO_3$ nanocrystals with tailored nanostructures by the ultrasonic method have been very scarce so far.

In this work, a simple and fast ultrasound irradiation method is developed to prepare $SrTiO_3$ particles with tailored nanostructures. Nanoporous $SrTiO_3$ particles are synthesized and their porous nature can be controlled by altering the experimental conditions. The formation mechanism of these nanoporous $SrTiO_3$ particles is briefly discussed. Furthermore, the rheological behavior of suspensions composed of nanoporous $SrTiO_3$ particles with different nanostructures is also studied.

2. Experimental details

2.1. Materials

Tetrabutyl titanate (TBT, >98%), hydrochloric acid (HCl) and sodium hydroxide (NaOH) were purchased from Sinopharm Chemical Reagent Company (Shanghai, China). Strontium hydroxide ($Sr(OH)_2{\cdot}8H_2O$) was obtained from Tianjin Guangfu Fine Chemical Research Institute (Tianjin, China). All chemicals were of analytical grade and used without further purification. Doubly deionized water was used throughout all the processes.

2.2. Synthesis of nanoporous $SrTiO_3$ crystals and electrorheological fluids

Mesoporous $SrTiO_3$ particles were synthesized by the ultrasonic irradiation method. In a typical synthesis, $Ti(OBu)_4$ (0.05 mol) was first dissolved in ethyl alcohol (15 ml) under continuous stirring at room temperature to form a yellow solution. Then, $Sr(OH)_2{\cdot}8H_2O$ (0.05 mol) was added to the solution. After being stirred for 10 min, doubly deionized water (70 ml) was added to the above container and a milky white suspension was obtained. Then, the reaction mixture under different pH values was irradiated with a high-intensity ultrasonic probe (from Xinzhi Co., China, JY92–2D, with a 6 mm diameter titanium horn of 20 kHz working in a pulsed mode with a duty cycle of 7 s) at room temperature in ambient air for 1 h. The final products were separated by centrifugation and washed several times with doubly deionized water and alcohol. Finally, the products were dried under a vacuum at 50 °C for 10 h.

The obtained $SrTiO_3$ particles were further dried at 120 °C for 3 h and then dispersed into silicone oil (density of ∼0.96 g cm^{-3}, viscosity of 500 cPa s at 25 °C) with mechanical stirring to form a uniform electrorheological fluid (ERFs).

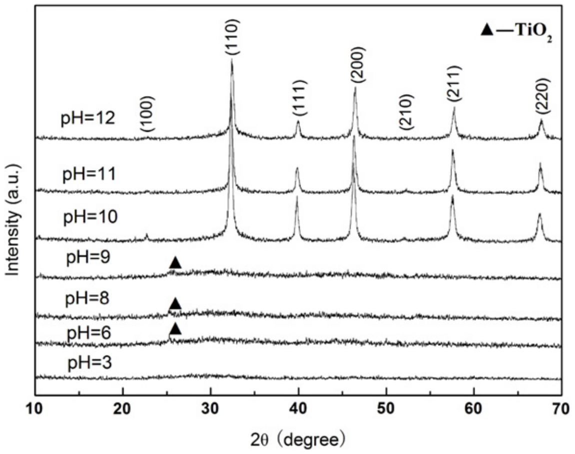

Figure 1. XRD curves of the as-prepared $SrTiO_3$ samples at different pH values.

2.3. Instruments

X-ray diffraction (XRD) patterns were obtained by a Rigaku diffactometer (MXPAHF, Japan) with Cu K_α radiation ($\lambda = 0.15406$ nm). The scanning rate of the diffactometer is 8° min^{-1}. The measurement was carried out by a generator with a voltage of 40 kV and a current of 100 mA. The nitrogen (N_2) adsorption/desorption isotherms at about 77 K were studied using a Micromeritics ASAP 2020M system. The morphology of the powders was observed with a scanning electron microscope (SEM, Sirion 200, Holland) operating at 5 kV. The microstructure of the particles was investigated by a transmission electron microscope (TEM, JEM-2100F, Japan). A rotational rheometer (Physica, MCR 301, Anton Paar, Austria, the gap between the outer barrel and the inner probe was 0.42 mm), with the ER HVS/ERD 180 and CC10-E accessories, was used to measure the rheological characteristics of the ERF, where the ERF was placed into the barrel between the two concentric probes. The rotational rheometer equipped with the temperature control accessory Physica VT 2 was used to measure the temperature dependence of shear stress.

3. Results and discussion

3.1. XRD characterization of nanoporous $SrTiO_3$ particles

In our system, nanoporous $SrTiO_3$ materials were synthesized by the hydrolysis of Sr alkoxide and a Ti source under ultrasound irradiation. $SrTiO_3$ particles with different nanostructures were synthesized by tuning the pH of reactions. Figure 1 shows the XRD patterns of the $SrTiO_3$ particles prepared under different pH values (pH = 3, 6, 8, 9, 10, 11 and 12), respectively. As shown in figure 1, the as-prepared nanoparticles were all amorphous when the pH < 10. However, when the pH is higher than 10, several diffraction peaks were clearly found in the XRD patterns and the position

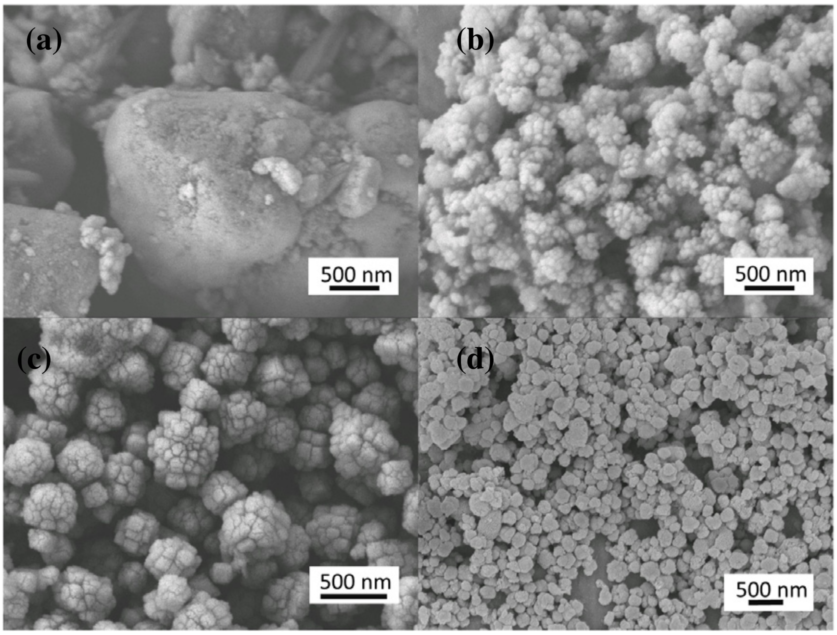

Figure 2. The surface morphology of as-prepared $SrTiO_3$ samples under different pH values ((a) pH = 9, (b) pH = 10, (c) pH = 11 and (d) pH = 12) viewed by SEM.

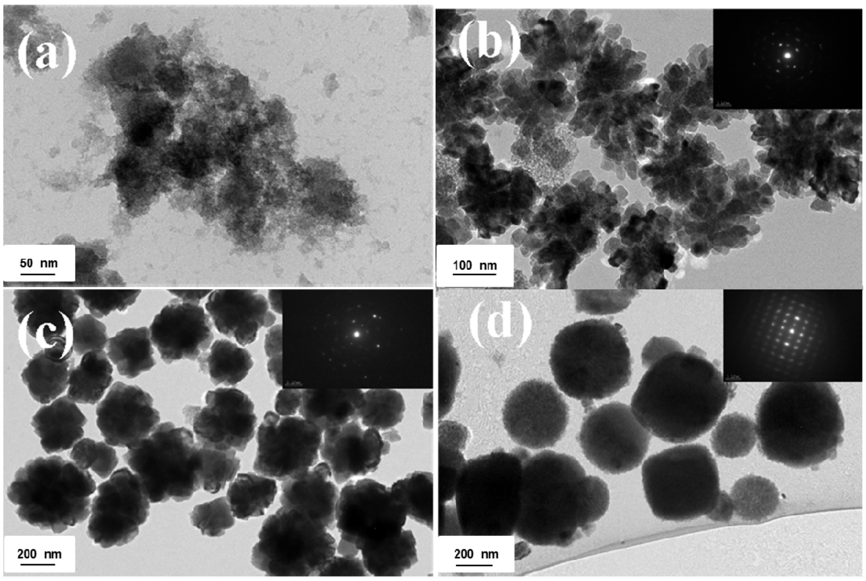

Figure 3. The microstructure of as-prepared $SrTiO_3$ samples under different pH values ((a) pH = 9, (b) pH = 10, (c) pH = 11 and (d) pH = 12) viewed by TEM. The inset shows the SAED images.

and relative intensity of all diffraction peaks match well with a cubic structure of $SrTiO_3$ (JCPDS 35-0704). Obviously, the as-prepared $SrTiO_3$ nanomaterial was well crystallized.

3.2. The effect of pH value

In this work, the influence of sonication power, sonication time and pH on the morphologies of $SrTiO_3$ materials was studied. The results showed that the influence of sonication power and sonication time could be neglected. However, we found that the morphology and crystalline nature of the $SrTiO_3$ particles were strongly dependent on the reaction pH value. As indicated by the XRD analysis, when the pH was lower than 10, the obtained $SrTiO_3$ was amorphous. In order to further investigate their morphology, SEM and TEM were conducted. Figures 2 and 3 show the SEM and TEM images of the $SrTiO_3$ nanomaterials which were synthesized under pH 10–12. It can be observed that the morphology of $SrTiO_3$ was flower-like, near-spherical and spherical, respectively, and the particle obtained at pH 12 was about 200 nm. These samples exhibited high crystallinity, which can be proved by the SAED images inserted in figure 3. In agreement with the XRD pattern, the $SrTiO_3$ particle prepared under pH 12 possessed excellent

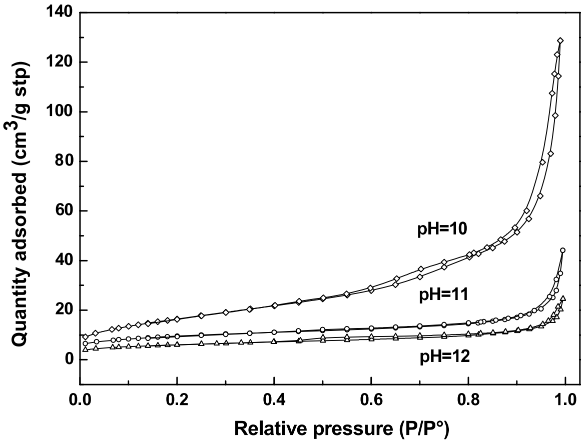

Figure 4. The nitrogen adsorption/desorption isotherms of as-prepared $SrTiO_3$ samples under different pH values.

crystallinity (figure 3(d)). In light of these results, it is very clear that $SrTiO_3$ particles with tunable nanostructures can be controllably synthesized via our ultrasonic irradiation method by tuning the experimental parameters.

3.3. Proposed growth mechanism

From the above analysis, we can find that the pH value of the solvent has a great effect on the morphology and crystalline nature of the final product. It is believed that the hydrolysis rate and the growth rate of crystallites are dominated by the pH value of the solution in this system. The crystalline nature and morphology of $SrTiO_3$ depend on the competition between the hydrolysis of the Ti salt and the condensation reaction of $SrTiO_3$. When the pH value of the solvent is less than 10, the hydrolysis speed is faster than that of growth. In this circumstance ($pH < 10$), the amorphous TiO_2 was firstly formed, followed by the formation of amorphous $SrTiO_3$. The likely reaction steps for the formation of amorphous $SrTiO_3$ nanoparticles are as follows:

$$Ti^{4+} + 2H_2O \rightarrow TiO_2 + 4H^+ \tag{1}$$

$$TiO_2 + Sr^{2+} + 2OH^- \rightarrow SrTiO_3 + H_2O. \tag{2}$$

However, when the pH is higher than or equal to 10, alkoxide ions react with water molecules to form the complex ion $[Ti(OH)_6]^{2-}$, which will neutralize with the Sr^{2+} ion, then polymerize to $Sr^{2+}[Ti(OH)_6]^{2-}$ and finally form crystalline $SrTiO_3$ (equations (3) and (4)) [23, 24]:

$$Ti^{4+} + 6OH^- \rightarrow [Ti(OH)_6]^{2-} \tag{3}$$

$$[Ti(OH)_6]^{2-} + Sr^{2+} \rightarrow SrTiO_3 + 3H_2O. \tag{4}$$

The crystallization of $SrTiO_3$ is promoted by ultrasonic irradiation. When the pH is between 10 and 12, fine crystallites are formed and then gather into flower-like grains (figure 3(b)) at lower pH values. Furthermore, with the increase of the pH value to 12, crystal agglomeration is enhanced, $SrTiO_3$ aggregation becomes near-spherical and the morphologies and crystalline nature became regular.

Table 1. The influence of pH value on the porosity and crystalline shape of $SrTiO_3$ sample. (Note: A, P and S represent amorphous, polycrystalline and single-crystalline, respectively. The sonication time and sonication power are kept as 100 min and 200 W, respectively.)

pH value	6	8	9	10	11	12
S_{BET} ($m^2\ g^{-1}$)	251.8	224.1	197.1	60.8	23.4	20.4
V_t ($cm^3\ g^{-1}$)	0.18	0.17	0.16	0.20	0.06	0.04
Pore size (nm)	4.2	4.1	4.5	12.3	12.1	10.2
Crystalline shape	A	A	A	P	P	S

3.4. Nanoporous nanostructure and their BET properties

From the XRD patterns, it is very clear that the diffraction peaks are relatively broad and not sharp. The TEM images also show that the as-prepared $SrTiO_3$ particles are composed of primary nanosized domains, which indicate that these products were porous. In order to provide direct proofs of their nanoporous nature, nitrogen adsorption/desorption isotherm characterizations were used. Figure 4 shows the BET specific surface area measurement results of the nanoporous $SrTiO_3$ samples which were prepared under different pH values (10–12). The curves show a single and narrow hysteresis loop. This may be due to the special one-end-open shape of the pore structure creating a similar initial pressure of evaporation and capillary condensation. Similar experimental results were also found in [25]. The BET specific surface areas (S_{BET}), total pore volumes (V_t) and pore diameters of the porous $SrTiO_3$ under different pH values are summarized in table 1. With the increase of the pH value, the BET specific surface areas decreased from 251.8 $m^2\ g^{-1}$ ($pH = 6$) to 20.4 $m^2\ g^{-1}$ ($pH = 12$). The total pore volume and the pore size had a maximum of 0.20 $cm^3\ g^{-1}$ and 12.3 nm when $pH = 10$. Thus, in our system, $SrTiO_3$ with different nanostructures and specific surface areas can be selectively obtained by adjusting the reaction pH.

3.5. Electrorheological properties of as-prepared $SrTiO_3$ ER suspension

Electrorheological fluid (ERF) is a kind of smart suspension consisting of high dielectric particles dispersed in an insulating liquid [26]. The properties of ERF can be easily controlled by application of an external electric field. They are generally considered to have many important applications in the automotive industry. In this work, the rheological behaviors of suspensions which were composed of $SrTiO_3$ particles suspended in silicone oil were also studied and $SrTiO_3$ particles synthesized under pH 10, 11 and 12 were used as the precursor, respectively.

Figures 5(a) and (b) showed the flow and viscosity curves for various suspensions under a fixed electric field strength of $E = 2$ kV mm^{-1}. The suspensions exhibited a shear stress that increases with the shear rate. Furthermore, the shear stress of $SrTiO_3$ERF (synthesized under pH 10) was conspicuously higher than that at $pH = 11$ or 12. As discussed above, the $SrTiO_3$ particles synthesized under higher pH show a lower BET area than those synthesized under lower pH values. In this system, the ER effect was dependent on the BET area,

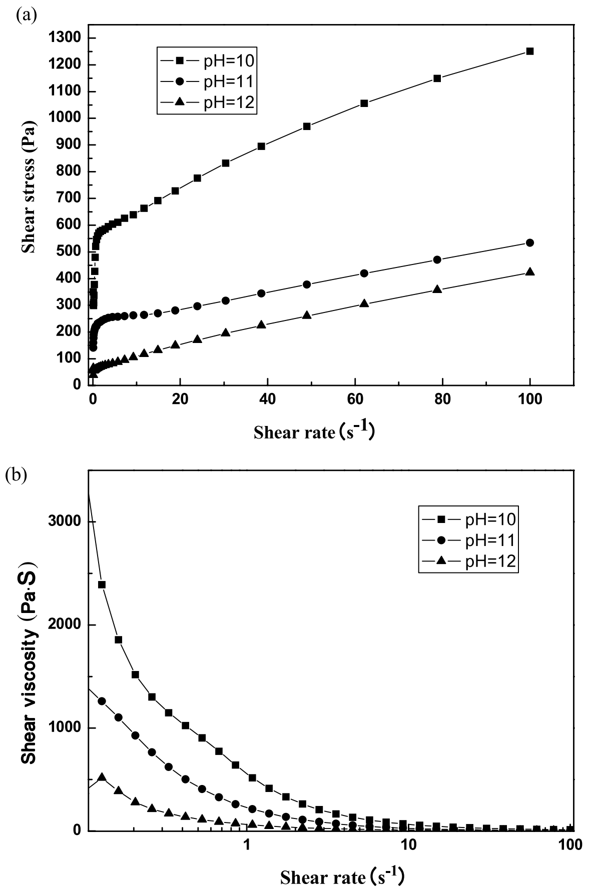

Figure 5. (a) Flow curves at a fixed strength, $E = 2$ kV mm^{-1}, of the applied electric field for various pH values (10, 11 and 12, respectively). (b) Corresponding curves of viscosity versus shear rate.

therefore the $SrTiO_3$ particles synthesized under lower pH show a higher ER effect than those synthesized under higher pH values. Moreover, because of larger specific surface areas, the particles synthesized under pH 10 had larger wettability and can be polarized easily. This resulted in higher ER activity. As shown in figure 5(b), due to the shear rate being larger than 1 s^{-1}, the suspensions indicated shear thinning behavior, which was a behavior commonly observed in ER fluids. Obviously, from the above analysis, we can conclude that as-prepared $SrTiO_3$ particles with different nanostructures can be used as the precursor for ERFs and higher BET $SrTiO_3$ particles often lead to higher ER effect materials.

4. Conclusions

In this study, a simple and efficient sonochemical method was developed for the synthesis of nanoporous $SrTiO_3$ crystals with different nanostructures and BET specific surface areas. Results showed that the morphology and crystalline nature of $SrTiO_3$ crystals were strongly pH-dependent. The nitrogen adsorption–desorption method indicated that the particles possessed a porous structure with high BET specific surface areas. As-prepared $SrTiO_3$ particles with different nanostructures can be used as the precursor for ERFs. Investigation on the electrorheological activities of ER suspensions demonstrated that the shear stress was dependent on the crystal nature of the $SrTiO_3$ particles and these suspensions showed shear thinning behavior. The design of controlling the pH value might open up new perspectives in preparing novel ER materials.

Acknowledgment

Financial support from the National Basic Research Program of China (973 Program, grant no. 2007CB936800) is gratefully acknowledged.

References

[1] Hu Y, Tan O K, Cao W and Zhu W 2004 *Ceram. Int.* **30** 1819
[2] Konta R, Ishii T, Kato H and Kudo A 2004 *J. Phys. Chem.* B **108** 8992
[3] Miyauchi M, Takashio M and Tobimatsu H 2004 *Langmuir* **20** 232
[4] Wang D F, Ye J H, Kako T and Kimura T 2006 *J. Phys. Chem.* B **110** 15824
[5] Lenzmann F, Krueger J, Burnside S, Brooks K, Gratzel M, Gal D, Ruhle S and Cahen D 2001 *J. Phys. Chem.* B **105** 6347
[6] Tao J T, Ma J F, Wang Y G, Zhu X Y, Liu J and Jiang X H 2006 *J. Am. Ceram. Soc.* **89** 3554
[7] Chen Y Y, Yu B Y, Wang J H, Cochran R E and Shyue J J 2009 *Inorg. Chem.* **48** 681
[8] Chen W P, Zhu Q A, Song F P and Wang S F 2006 *Chinese J. Inorg. Chem.* **22** 2105
[9] Xie J, Ji T H, Ou-Yang X H, Mao Z Y and Shi H J 2008 *Solid State Commun.* **147** 226
[10] Larsen G, Lotero E, Nabity M, Petkovic L M and Shobe D S 1996 *J. Catal.* **164** 246
[11] Stone F V and Davis R J 1998 *Chem. Mater.* **10** 1468
[12] Corma A 1997 *Chem. Rev.* **97** 2373
[13] Wang Y W, Xu H, Wang X B, Zhang X, Jia H M, Zhang L Z and Qiu J R 2006 *J. Phys. Chem.* B **110** 13835
[14] Zhou N, Chen G, Xian H Z and Zhang H J 2008 *Mater. Res. Bull.* **43** 2554
[15] George C N, Thomas J K, Jose R, Kumar H P, Suresh M K, Kumar V R, Shobana Wariar P R and Koshy J 2009 *J. Alloys Compounds* **486** 711
[16] Chen W, Cai W P, Lei Y and Zhang L D 2001 *Mater. Lett.* **50** 53
[17] Xu M, Lu Y N, Liu Y F, Shi S Z and Fang F 2006 *J. Am. Ceram. Soc.* **89** 3631
[18] Li H, Ni Y H and Hong J M 2009 *Scr. Mater.* **60** 524
[19] Suslick K S, Choe S B, Cichowlas A A and Grinstaff M W 1991 *Nature* **353** 414
[20] Okitsu K, Mizukoshi Y, Bandow H, Maeda Y, Yamamoto T and Nagata Y 1996 *Ultrason. Sonochem.* **3** S249
[21] Hyeon T H, Fang M M and Suslick K S 1996 *J. Am. Chem. Soc.* **118** 5492
[22] Okawa H, Yabuki J, Kawamura Y, Arise I and Sato M 2008 *Mater. Res. Bull.* **43** 1203
[23] Harizanov Q A 1998 *Mater. Lett.* **34** 345
[24] Kavian R and Saidi A 2009 *J. Alloys Compounds* **468** 528
[25] Hou R Z, Ferreira P and Vilarinho P M 2008 *Micropor. Mesopor. Mater.* **110** 392
[26] Parmar K P S, Meheust Y, Schjelderupsen B and Fossum J O 2008 *Langmuir* **24** 1814